HHS Public Access

Author manuscript

Nanomedicine. Author manuscript; available in PMC 2018 May 01.

Published in final edited form as:

Nanomedicine. 2017 May ; 13(4): 1495–1506. doi:10.1016/j.nano.2016.12.019.

Mechanisms that determine nanocarrier targeting to healthy versus inflamed lung regions

Jacob S. Brenner[†,‡], **Kartik Bhamidipati**[‡], **Patrick M. Glassman**[‡], **N. Ramakrishnan**[§], **Depeng Jiang**[#], **Andrew J. Paris**[†], **Jacob W. Myerson**[‡], **Daniel C. Pan**[‡], **Vladimir V. Shuvaev**[‡], **Carlos H. Villa**[‡], **Elizabeth D Hood**[‡], **Raisa Kiseleva**[‡], **Colin F. Greineder**[‡], **Ravi Radhakrishnan**[§], and **Vladimir R. Muzykantov**[‡,*]

[†]Pulmonary and Critical Care Division, University of Pennsylvania, Philadelphia, PA 19104, USA

[‡]Department of Pharmacology and Center for Translational Targeted Therapeutics and Nanomedicine, Perelman School of Medicine, University of Pennsylvania, Philadelphia, PA 19104, USA

[§]Department of Bioengineering, University of Pennsylvania, Philadelphia, PA 19104, USA

[#]Department of Respiratory Medicine, The Second Affiliated Hospital, Chongqing Medical University, Chongqing, China

Abstract

Inflamed organs display marked *spatial heterogeneity* of inflammation, with patches of inflamed tissue adjacent to healthy tissue. To investigate how nanocarriers (NCs) distribute between such patches, we created a mouse model that recapitulates the spatial heterogeneity of the inflammatory lung disease ARDS. NCs targeting the epitope PECAM strongly accumulated in the lungs, but were shunted away from inflamed lung regions due to hypoxic vasoconstriction (HVC). In contrast, ICAM-targeted NCs, which had lower *whole-lung* uptake than PECAM/NCs in inflamed lungs, displayed markedly higher NC levels in inflamed *regions* than PECAM/NCs, due to increased regional ICAM. Regional HVC, epitope expression, and capillary leak were sufficient to predict intra-organ of distribution of NCs, antibodies, and drugs. Importantly, these effects were not observable with traditional spatially-uniform models of ARDS, nor when examining only whole-organ uptake. This study underscores how examining NCs' *intra-organ* distribution in spatially heterogeneous animal models can guide rational NC design.

Graphical abstract

*Corresponding Author: Address correspondence to muzykant@mail.med.upenn.edu.

AUTHOR INFORMATION

Author Contributions

The manuscript was written through contributions of all authors. All authors have given approval to the final version of the manuscript.

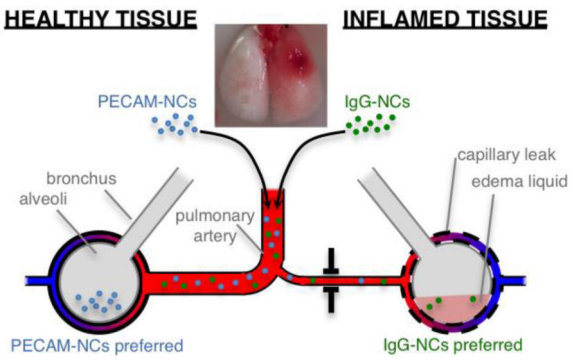

To understand how nanocarriers (NCs) distribute between inflamed vs healthy tissue, we created a mouse model in which just one lobe of the lung is severely inflamed (inset photo). We found that highly lung-avid NCs (PECAM/NCs) preferentially accumulate in the *healthy* lung tissue, due to hypoxic vasoconstriction in the inflamed tissue. Surprisingly, untargeted NCs (IgG/NCs) accumulate in the *inflamed* tissue, due to capillary leak there. These experimental findings, along with computational modeling, allowed us to design a highly lung-avid NC that also preferentially targets the inflamed tissue.

Keywords

Spatial heterogeneity; patchy; inflammation; ARDS; nanoparticles; nanocarriers; nanoparticle biological interactions; whole organ distribution; nano-bio interface

BACKGROUND

Nanomedicine has made great progress in targeting nanocarriers (NCs) to individual organs [1– 5] . However, within an organ, diseases display a large degree of *spatial heterogeneity*, with the same organ containing both healthy and pathological regions [6–10]. Thus, some NCs may appear to efficiently target an organ, but it remains unknown if those NCs in fact target the pathological subregions rather than the nearby healthy regions. To address this question, a major need exists for animal models which recreate the spatial heterogeneity seen in human diseases.

Therefore, we created a new mouse model to study how NCs distribute within a diseased organ that displays the spatial heterogeneity typical of human diseases. We chose to focus on inflammatory disorders, since they constitute a very large class of diseases, change organ physiology significantly, and nearly all display spatial heterogeneity in their severity. We chose as our model inflammatory disease ARDS (acute respiratory distress syndrome), which is an acute, diffuse, inflammatory lung injury that kills ~75,000 Americans annually [11]. In ARDS, the capillaries of the lungs' alveoli (air sacs) increase their permeability, causing the alveoli to fill with edema liquid and neutrophils [12], similar to the leukocyte-rich tissue edema present in nearly all inflammatory diseases. Notably, in every ARDS patient, these inflammatory changes are only found in scattered patches of the lung[13, 14], making ARDS an archetype of spatially heterogeneous organ inflammation. Targeting these inflamed lung regions has been the goal of numerous labs' NCs and a program to develop

liposomal drug delivery for ARDS [15–19], but these NC studies only examined whole lung uptake, and not whether the NCs actually reached the inflamed lung regions.

For the present study, we initially focused on the most-studied of these NCs: NCs coated with anti-PECAM antibodies (PECAM/NCs), which have shown very high whole lung uptake in ARDS models in mice, rats, and pigs [18, 20, 21]. In our mouse model of spatially heterogeneous ARDS, we found that PECAM/NCs accumulate preferentially in healthy lung regions, not the intended inflamed lung regions, due to hypoxic vasoconstriction. Surprisingly, however, we found that other NCs and pharmacological agents actually preferentially accumulated in the inflamed lung regions. Experimental and computational studies showed that these diverse distributions were determined by 3 simple transport mechanisms, which allowed us to design a new targeted NC, ICAM/NC, that shows strong preference for the most inflamed regions. Notably, ICAM/NCs appear inferior to PECAM/NCs in traditional, spatially-uniform ARDS models, with lower whole-lung uptake than PECAM/NCs even in inflamed lungs. Only by comparing ICAM/NCs vs. PECAM/NCs in a spatially heterogeneous animal model and examining intra-organ distribution did it become clear that ICAM/NCs achieve higher *local* concentrations in the inflamed areas in need of pharmacotherapy. These findings highlight the importance of developing spatially heterogeneous animal models like the one introduced here.

METHODS

Unilateral LPS instillation

C57BL/6 adult mice were instilled with LPS (1 mg/kg). For the traditional “diffuse LPS” model of ARDS, the LPS was instilled via insertion of a 29-gauge tuberculin syringe into the trachea. For unilateral LPS, the mice were anesthetized with ketamine and xylazine followed by endotracheal intubation with a 20-gauge angiocatheter. A PE-10 catheter (outer diameter 0.024”) was inserted and positioned so that it terminated within the superior lobe, and the LPS was instilled as a 1 uL / kg solution. Twenty-four hours later, assays of lung distribution (NC injection followed by sacrifice 30 minutes later) and lung inflammation were performed as previously described [22].

Nanoparticle production

Liposomes were made by first creating lipid films in round-bottom glass vials: 1×10–5 moles of lipids in chloroform were added per vial, followed by chloroform evaporation via nitrogen stream and then at least 2 hours of lyophilization . Lipids (from Avanti) were mixed at molar percent: DPPC 52%, cholesterol 45%, DSPE-PEG-2000-maleimide 2%, with the remaining 1% being either DSPE-PEG-2000-DTPA (for In^{111} labeling experiments), PE-lissamine-rhodamine (for fluorescent tracing), or DPPC (for all other experiments). Lipid films then had 0.5 mL PBS added, warmed to 50C, bath sonicated at 50C for 10 seconds, followed by extrusion (Avanti syringe extruder) through a membrane with 200-um pores, producing ~2×10^{13} liposomes / mL [18].

Antibodies were conjugated to maleimide-liposomes by SATA-maleimide conjugation chemistry. Briefly, a 6x excess of SATA (Sigma) was added to antibodies at room

temperature (RT) for 30 min, generating 1 sulfhydryl group per IgG molecule. The acetylated sulfhydryl of the SATA moiety by adding hydroxylamine (50 mM final concentration) and incubating for 2 hours at RT. Then maleimide-containing liposomes were mixed with the deprotected SATA-antibodies to generate liposomes that bore approximately 200 antibodies per liposome [18]. Unconjugated antibodies were removed by centrifugation at 32,000 x *g* for 1 hour to pellet the conjugated liposomes, and discarding the supernatant containing free antibodies.

The liposomes were radiolabeled with I^{125} as described previously [18]: 10% of their coating antibodies be I^{125}-labeled IgG. I^{125}-labeling of IgG utilized Pierce iodination beads, conducted after SATA-conjugation to the antibodies.

For digital autoradiography (DAR), liposomes containing 1% DSPE-PEG-2000-DTPA were labeled with In^{111}: In111 source (150 uCi; from Nuclear Diagnostics Products) was mixed with 2M trimethyl acetic acid (pH 4.5) and pH set to 4.5, and then mixed at with antibody-conjugated liposomes at a volume ratio of 2:1 liposomes:In^{111}-TMAA, incubated at room temperature for 1 hour, and then centrifuged at 32,000xg for 1 hour. In111 loading showed: 91% of the In111 was found in the pellet, and on thin layer chromatography (TLC) in 2 different mobile phases (9% NaCl, 10 mM NaOH; and 10 mM EDTA), 99% of the In111 migrated with the liposomes in both mobile phases.

Nanogels (lysozyme-dextran nanogels of 300 nm) were produced via the method previously described [23].

Nanoparticle tracing *in vivo*

For multi-organ biodistribution, mice were injected with 2×10^{11} liposomes / mouse, which is equivalent to 5 mg/kg of total lipid. Nanogel injections were similarly $\sim 1 \times 10^{11}$ nanoparticles per mouse.

Digital autoradiography (DAR) was performed by injecting the mice with In^{111}-labeled liposomes. These liposomes contained 1% sacrifice 30 minutes later, and preparation of fresh-frozen lungs in OCT. Lung blocks were cut on a cryostat microtome, with the slides then developed on a phosphor screen plate overnight followed by imaging the screen on a Typhoon FL7000.

Fluorescent liposomes were injected and the lungs prepared identically for those of In^{111}-labeled liposomes. Fluorescent images were taken on an Aperio slide scanner.

Tc99m–MAA (macroaggregated albumin) was purchased from Nuclear Diagnostics Products, and injected into mice in a volume of 100 uL of PBS containing on average 350 MAA particles.

RESULTS

Development of a mouse model to test how NCs distribute to healthy vs. inflamed lung regions

In human ARDS, inflamed lung regions display a number of changes (Fig 1A): the air sacs (alveoli) fill up with edema liquid and neutrophils, the capillaries surrounding the air sacs increase their permeability ("capillary leak"), and the arterioles leading to such air sacs constrict ("hypoxic vasoconstriction") [12, 24, 25]. Therefore, we developed a mouse model that displays each of these features, in the spatially heterogeneous pattern characteristic of human ARDS (Fig 1B–E).

We call this mouse model the "unilateral LPS model" because of the procedure used to induce the spatially heterogeneous ARDS-like phenotypes. During the procedure (Fig 1B), a catheter (green line) is inserted through the mouse's mouth and into the superior lobe of the right lung, where lipopolysaccrhide (LPS; a bacterial cell wall toxin) is instilled (Fig 1B). The result is that one lung region displays severe ARDS-like inflammation (the superior lobe of Fig 1C), while the rest of the lungs remain healthy (see the left lung of Fig 1C). The most striking hallmarks of human ARDS are the capillary leak and the ensuing leakage of edema liquid into the lung. The model recapitulates this well, with the inflamed superior lobe displaying a 2.5-fold increase in weight, due to the alveoli being filled with edema liquid (Fig 1D), similar to 2–3-fold increase in lung weight in human ARDS[26]. By contrast, in the most commonly used animal model of ARDS, in which LPS is diffusely sprayed throughout the lungs (the "diffuse LPS" model), there is no statistically significant increase in weight of either the superior lobe or left lung (Fig 1D, orange bars). The final phenotype of ARDS that the unilateral LPS mice recapitulates is neutrophilic infiltration (Fig 1E), which is severe in the superior lobe, but absent in the left lung (with the left lung indistinguishable from the lungs of naive mice). Thus, the unilateral LPS model displays the major features of spatially heterogeneous ARDS and thus may serve as a test bed for determining where NCs and drugs distribute within the lung.

PECAM/NCs strongly accumulate in the lungs, but preferentially accumulate in the healthy regions of ARDS-affected lungs

Having established our mouse model of spatially heterogeneous ARDS, we next tested the distribution of PECAM/NC within the lungs of mice. We first constructed liposomes coated with anti-PECAM antibodies (PECAM/liposomes; see Supplemental Figure 1A for characterization, such as size distribution). We then determined how strongly the PECAM/liposomes target the lungs by injecting into healthy (naïve) mice I^{125}-labeled PECAM/liposomes and 30 minutes later harvesting the organs. As shown in Figure 1A, PECAM/liposomes accumulate in the lungs at 183% of the injected dose per gram of tissue (%ID/g), thus achieving much higher tissue concentrations in the lungs than all other organs and at accumulating in the lung 5.9-fold more than control IgG/liposomes. Therefore, PECAM/liposomes can serve as a paradigm for IV NCs which achieve marked uptake in the lungs.

Having shown that PECAM/liposomes achieve strong uptake in the whole lungs of healthy mice, we next sought to determine how they distribute between inflamed and healthy regions

in mice that underwent unilateral LPS. After LPS instillation, 24 hours later we intravenously injected I^{125}-labeled PECAM/liposomes, sacrificed the mice 30 minutes later, and then measured the uptake in all 5 lung lobes via a gamma counter (Fig 2B,C). As seen in Figure 2B, when measuring PECAM/liposomes uptake as the percent of injected dose per organ (%ID, here "organ" refers to a single lung lobe), there is no statistically significant difference in PECAM/NC uptake in the left lung between naive mice, the classical model of diffuse LPS, and unilateral LPS mice. However, in the inflamed superior lobe of unilateral LPS mice, the normalized %ID/organ of the superior lobe is 0.57, suggesting that the inflamed superior lobe of unilateral LPS mice gets only 57% the mass of PECAM/liposomes received by the superior lobe of naive mice, which suggests shunting of PECAM/liposome mass away from the inflamed superior lobe.

More important than comparing the superior lobes of naive mice versus unilateral LPS mice is determining *within an individual unilateral LPS animal* whether PECAM/NCs are shunted away from the inflamed superior lobe and instead go towards the healthy left lung. To quantify this, we introduce the ***PATH ratio*: the Pathologically Altered To Healthy tissue ratio**. The PATH ratio is defined for an *individual* animal as being the ratio of NC mass in the pathologically altered tissue to the nanocarrier mass in healthy tissue. In this particular experiment, the PATH ratio is for a unilateral LPS mouse the %ID/organ of PECAM/NC in the pathologically most altered tissue (the inflamed superior lobe) divided by the %ID/organ in the healthiest tissue (left lung). Because the superior lobe and left lung are not the same size, we present the PATH ratio as normalized to the same ratio obtained in naive mice. In Figure 2C we have plotted the ratio of %ID/organ of the superior lobe to left lung, comparing naive mice vs. diffuse LPS vs. unilateral LPS (all normalized to naive). In this plot, the bar for unilateral LPS represents, by definition, the PATH ratio for PECAM/NC. As seen in Fig 3D, the PATH ratio for PECAM/liposomes is 0.55, which indicates that the most inflamed lung region (the superior lobe) receives only 55% the mass of PECAM/liposomes that the healthiest region (left lung) receives. Thus, spatially heterogeneous ARDS-like injury causes strong shunting of PECAM/NCs away from the tissue most in need of pharmacotherapy.

To test whether this effect is specific to liposomes, we conducted the same experiment with another translationally-relevant nanocarrier, lysozyme-dextran nanogels ("nanogels" see Supplemental Fig 2A for characterization). Like PECAM/liposomes, PECAM/nanogels strongly accumulate in the lungs (130%ID/g; 7.9-fold higher than control nanogels; see Supplemental Figure 2). As with PECAM/liposomes, PECAM/nanogels display in unilateral LPS mice a PATH ratio significantly less than 1 (Fig 2D, right bar), suggesting marked shunting of PECAM/nanogels away from the most inflamed tissue. Importantly, this shunting of PECAM/NCs (PATH < 1) was seen in two different NCs (liposomes vs nanogels) that show markedly different pharmacokinetics, with the time to reach peak lung concentrations differing by at least 25 minutes and much slower clearance of the blood pool for PECAM/liposomes (Supplmental Fig 1B vs Supplemental Fig. 2C). Thus the shunting effect for PECAM/NCs seems to be largely independent of the particular NC formulation. Therefore, hereafter all NCs used were liposomes.

Finally, we sought to ensure that these differences in regional lung uptake of PECAM/NC were not due to LPS-induced changes in *overall* lung uptake of NCs. As displayed in Figure 2E, for PECAM/liposomes, the %ID / organ in the lung was ~25%, regardless of the presence of diffuse or unilateral LPS. Also, PECAM/nanogels had significantly lower overall lung uptake (%ID/organ = 19%) than PECAM/liposomes, but still had very similar PATH ratio values. Thus, the regional shunting of PECAM/NC from the most pathologically altered lung region is not a byproduct of changes in overall lung uptake.

PECAM/NCs are shunted away from inflamed lung regions largely due to hypoxic vasoconstriction

To explain the marked shunting of PECAM/NCs, we hypothesized it was caused by decreased local blood flow to the inflamed lung region (superior lobe). In animals[27] and humans with ARDS[14], *hypoxic vasoconstriction* has been frequently observed: constriction of the arteriole feeding hypoxic regions of th lung. To assess for hypoxic vasoconstriction, we measured blood flow in our unilateral LPS model using the same probe as used in the clinical studies of regional lung blood flow: Tc^{99m}-MAA (technetium^{99m}-labeled macroaggregated albumin) [28]. When injected intravenously, the 20–70 um diameter Tc^{99m}-MAA particles immediately lodge in the 6–8 um pulmonary capillaries. The relative uptake of Tc^{99m}-MAA in each pulmonary lobe is directly correlated with relative blood flow to that lobe.

Compared to naive mice, the blood flow (relative Tc^{99m}-MAA signal) in unilateral LPS mice increases slightly in the healthy left lung, and is decreased by about half in the inflamed superior lobe (Fig 3A). We next calculated for each animal the ratio of Tc^{99m}-MAA in the most inflamed region (superior lobe) to healthy region (left lung) (Fig 3B). The value for unilateral LPS mice on such a plot is, by definition, the PATH ratio value for Tc^{99m}-MAA, here 0.52. Note how the PATH ratio value of Tc^{99m}-MAA (0.52) is nearly identical to that of PECAM/NC (0.55; Fig 3B, rightmost bar).

To further demonstrate the extremely strong correlation of blood flow (Tc^{99m}-MAA) and PECAM/NC, in Figures 3C and 3D we plotted the percent of total lung uptake for *all 5 lung lobes* for both Tc^{99m}-MAA (Fig 3C) and PECAM/NC (Fig 3D). These plots are nearly identical, for all lobes. For the region of greatest focus, the superior lobe, the relative blood flow (Tc^{99m}-MAA) goes from 19% to 11% comparing naive and unilateral LPS animals. For PECAM/NC, the superior lobe uptake also goes from 19% to 11%. Such a strong correlation between blood flow shunting and PECAM/NC shunting implies that PECAM/NCs distribute preferentially in healthy lung tissue due to decreased blood flow to pathological tissue.

PECAM/NCs preferentially accumulate in healthy lung tissue not only at the level of lung lobes, but also at the sub-lobar level

Having found that differences in inflammatory severity on the level of *whole lung lobes* strongly affect NC distribution, we next wanted to find out if heterogeneity in inflammation affects NC distribution between different regions *within a lobe*. This question is clinically relevant because in human ARDS there is heterogeneity of inflammation at the lobar level,

but even more prominently there is heterogeneity between immediately adjacent alveoli and acini (clusters of alveoli) [14].

To address this question, we used digital autoradiography (DAR) and immunofluorescence (IF) to image spatial distribution of PECAM/NC labeled either with In^{111} or rhodamine. DAR (Fig 4A) shows marked heterogeneity of PECAM/NC accumulatino at the sub-lobar level, negatively correlating with severity of sub-lobar inflammation. IF shows a similar pattern (Fig 4B).

IgG/NCs and untargeted agents accumulate preferentially in inflamed tissue

Having found that PECAM/NC are strongly shunted away from the inflamed superior lobe, we next sought to confirm that this property is shared by non-avid nanoparticles and other drug-like agents. Quite surprisingly, every *untargeted* agent we tested had a PATH ratio > 1, including IgG/NC, free IgG, and small molecule drugs. A PATH > 1 means they accumulated *preferentially in inflamed tissue*, the *opposite* direction of PECAM/NCs (Fig 5). Importantly, the gold standard for measuring capillary leak, radiolabeled albumin, also had a PATH ratio > 1, showing untargeted agents distribution correlates with capillary leak.

The finding that PECAM/NCs are unique among tested agents for having a PATH ratio < 1 appears to make such NCs unattractive for targeted drug delivery to the pathological regions of ARDS. However, while agents without lung avidity have much lower overall lung uptake than PECAM/NCs (Fig 2A). The combination of the two effects, PATH ratio and overall lung uptake, ultimately determines which agents achieve the best delivery to the flooded alveoli. To quantify this, we measured the percent of the injected dose (%ID) that ends up in the inflamed superior lobe, and found that PECAM/NCs massively outperform the other agents (Fig 5C): PECAM/NCs have a %ID in the inflamed superior lobe of 2.9%, compared to only 0.19% for the small molecule drug DTPA, a 15-fold difference in favor of PECAM/NCs.

ICAM/NCs preferentially accumulate in the inflamed lung regions, due to increased ICAM epitopes in ARDS-affected regions

While PECAM/NCs achieve remarkable delivery to the lungs, their accumulation at the intended site of therapy is markedly inhibited by their PATH ratio of 0.55. We hypothesized that we could overcome the effect of hypoxic vasoconstriction and blood-flow-shunting by coating our NCs with an antibody that binds an epitope that is increased in availability in inflamed lung tissue. Therefore, we performed a rapid screen to identify such epitopes. We induced lung inflammation with intravenous LPS, and then performed Western blots on whole lung homogenate, testing seven of the most studied lung-targeting epitopes. Only VCAM and ICAM showed upregulation in inflammation (Figure 6A), consistent with prior reports [29, 30]. We hereafter focused on ICAM because ICAM/NCs had much higher overall lung uptake than VCAM/NCs (data not shown).

Since ICAM protein levels increase in inflamed lungs, we next tested whether ICAM/NCs similarly increase uptake in the lungs. As shown in Figure 6B, compared to naïve mice, both diffuse LPS and unilateral LPS increase ICAM/NC uptake in whole lungs by ~25%. However, this inflammation-induced increase still leaves ICAM/NCs with ~15% *lower*

whole-lung uptake than PECAM/NCs (Fig 6B, comparing the two *orange bars*). Thus, using the traditional method of only examing *whole-lung* uptake does *not* indicate any drug-targeting advantage to using ICAM rather than PECAM targeting.

While ICAM-targeting did not have an advantage over PECAM-targeting at the whole organ level, we hypothesized that within heterogenously inflamed lungs, ICAM/NCs would preferentially accumulate in inflamed rather than healthy *regions*. Therefore, we built a multi-compartment pharmacokinetic (PK) computational model to predict if the mechanisms posited thus far were sufficient to produce the observed phenomena and predict the distribution of ICAM/NCs. As described in Supplemental Materials, the PK model showed that hypoxic vasconstriction and capillary leak were *sufficient* to produce the phenomena observed so far. Additionally, the PK model *predicted* that ICAM/NCs would have a PATH ratio ~1, providing the advantage over PECAM/NCs that we had hypothesized (Fig 6C).

Experimentally, we found that ICAM/NCs displayed a PATH ratio of 1.75 (Fig 6D, third bar), which is close to that of IgG/NCs and nearly the inverse of the low PATH ratio of PECAM/NCs. While other pharmacological agents we tested also had PATH ratio values > 1, none of them had strong overall lung uptake. However, ICAM/NCs had a %ID in the lung of 20.1%, just slightly lower than the 26.2% of PECAM/NCs (Fig 6E). Because of its high PATH ratio and moderately high overall lung uptake, ICAM/NCs displayed the highest uptake of all agents in the most inflamed lung region (superior lobe), with 4.9% of the injected dose going to the superior lobe, compared to 2.9% for PECAM/NCs (Fig 6F). By comparison, IgG/NCs and the model small molecule drug DTPA accumulated in the superior lobe at just 0.19% ID (Fig 5C), indicating ICAM/NCs provide a 26-fold improvement in delivery to the most inflamed lung tissue. Thus, switching to the appropriate antibody on a NC is able to overcome blood flow shunting and produce tremendous concentration in the pathologically altered tissue.

DISCUSSION

Targeting NCs to a diseased organ may be insufficient, as diseased organs usually have regions of healthy tissue intermixed with pathological regions, and NCs may preferentially accumulate in the healthy patches of tissue. To study this largely unexplored area of nanomedicine, we created a mouse model of the spatially heterogeneous inflammatory lung disease ARDS and analyzed how NCs distribute within the lungs.

The major generalizable finding from these studies is that analyzing *intra-organ* distribution of NCs in spatially heterogeneous disease models can elucidate properties of NC-targeting that are *not observable* in traditional models (which have homogeneous pathology and analyze only whole-organ uptake). This is well illustrated by the example of how the spatially heterogeneous ARDS model shows a superiority of ICAM/NCs over PECAM/NCs that was not observable with the traditional spatially-uniform model: At the whole-lung level, ICAM/NCs have significantly lower whole-lung uptake than PECAM/NCs, even in inflamed lungs (Fig 6B). This alone would suggest that PECAM/NCs are superior to ICAM/NCs for delivery to inflamed lungs. Surprisingly, though, the spatially heterogeneous ARDS (unilateral LPS) leads us to the *opposite conclusion*: ICAM/NCs are superior to

PECAM/NCs at delivery to inflamed lung *regions* (Fig 6F). Indeed, the inflamed lung region received about ~70% higher ICAM/NC levels than PECAM/NCs (Fig 6F). Since the goal with most ARDS drugs is to act solely on the inflamed regions, not the whole lung, the clinically-relevant parameter for NCs is accumulation in inflamed lung regions, not whole-lung accumulation. Therefore, the conclusion from the spatially heterogeneous model is more clinically-relevant than the misleading conclusion that can be drawn from whole-organ analysis of homogenous models.

To understand the disparity between ICAM/NC and PECAM/NC distribution, we investigated the mechisms which underlie NC distribution in heterogeneously inflamed lungs. We identified 3 *regional* mechanisms which appear sufficient to explain the diverse intra-pulmonary distributions observed here: *1)* regional hypoxic vasoconstriction (HVC; Fig 3); *2)* regional capillary leak (Fig 5); and *3)* regional change in epitope concentration in inflamed tissue (Fig 6). Figure 7 summarizes how each of these regional pathological changes affects NC distribution, using as examples NCs coated with either anti-PECAM, -ICAM, or untargeted IgG. Since the effects of 3 mechanisms on 3 different NCs in a dynamical system can be difficult to analyze with intution alone, we built a multi-compartment pharmacokinetic (PK) computational model (see Supplemental Materials). This PK model showed that these 3 mechanisms alone were sufficient to account for all the phenomena presented above.

The preference of some NCs for healthy instead of inflamed lung tissue (e.g., PECAM-NCs) has two important implications for therapeutic index. First, preferential accumulation in healthy tissue as seen in PECAM-NCs means that an increased mass of drug must be injected in order to deliver a therapeutic mass to inflamed lung. Second, many ARDS candidate drugs have direct toxcities on healthy lung tissue. For example, the two most clinically studied ARDS drugs, dexamethasone and albuterol, each ameliorate alveolar edema in ARDS, but they decrease neutrophil function and so would leave the healthy lung regions at increased risk of ventilator-associated pneumonia, an already common complication after ARDS. Therefore, there is clear benefit to designing NCs that preferentially target inflamed instead of healthy lung regions.

In summary, the field of Nanomedicine can benefit from studying how NCs and drugs distribute within spatially heterogenous diseased organs, as such studies can provide surprising results that can guide NC design and strategy.

Supplementary Material

Refer to Web version on PubMed Central for supplementary material.

Acknowledgments

J.S.B. was supported by NIH F32 HL 129665 - 01. D.C.P was supported by NIH T32 HL07915. Support for N.R, R.R, and V.R.M. by NIH U01EB016027. This study was supported in part by NIH via grants to V.R.M. (HL087036, HL090697 and HL121134).

ABBREVIATIONS

PATH ratio	Pathologically Altered To Healthy tissue ratio
NC	nanocarrier
PECAM	platelet endothelial cell adhesion molecule-1
ICAM	intercellular cell adhesion molecule-1
ARDS	acute respiratory distress syndrome

REFERENCES

1. Uddin MJ, Werfel TA, Crews BC, Gupta MK, Kavanaugh TE, Kingsley PJ, et al. Fluorocoxib A loaded nanoparticles enable targeted visualization of cyclooxygenase-2 in inflammation and cancer. Biomaterials. 2016; 92:71–80. [PubMed: 27043768]
2. Zhou H-F, Yan H, Hu Y, Springer LE, Yang X, Wickline SA, et al. Fumagillin prodrug nanotherapy suppresses macrophage inflammatory response via endothelial nitric oxide. ACS Nano. 2014; 8:7305–7317. [PubMed: 24941020]
3. Nguyen MM, Carlini AS, Chien M-P, Sonnenberg S, Luo C, Braden RL, et al. Enzyme-Responsive Nanoparticles for Targeted Accumulation and Prolonged Retention in Heart Tissue after Myocardial Infarction. Adv Mater. 2015; 27:5547–5552. [PubMed: 26305446]
4. Pan D, Pham CTN, Weilbaecher KN, Tomasson MH, Wickline SA, Lanza GM. Contact-facilitated drug delivery with Sn2 lipase labile prodrugs optimize targeted lipid nanoparticle drug delivery. Wiley Interdiscip Rev Nanomed Nanobiotechnol. 2016; 8:85–106. [PubMed: 26296541]
5. Kowalski PS, Kuninty PR, Bijlsma KT, Stuart MCA, Leus NGJ, Ruiters MHJ, et al. SAINT-liposome-polycation particles, a new carrier for improved delivery of siRNAs to inflamed endothelial cells. Eur J Pharm Biopharm. 2015; 89:40–47. [PubMed: 25460585]
6. Hiley CT, Swanton C. Spatial and temporal cancer evolution: causes and consequences of tumour diversity. Clin Med. 2014; 14(Suppl 6):s33–s37.
7. Weidenbusch M, Anders H-J. Tissue microenvironments define and get reinforced by macrophage phenotypes in homeostasis or during inflammation, repair and fibrosis. J Innate Immun. 2012; 4:463–477. [PubMed: 22507825]
8. Aird WC. Spatial and temporal dynamics of the endothelium. J Thromb Haemost. 2005; 3:1392–1406. [PubMed: 15892866]
9. González-García I, Solé RV, Costa J. Metapopulation dynamics and spatial heterogeneity in cancer. Proc Natl Acad Sci U S A. 2002; 99:13085–13089. [PubMed: 12351679]
10. Ju J, Li R, Gu S, Leader JK, Wang X, Chen Y, et al. Impact of emphysema heterogeneity on pulmonary function. PLoS One. 2014; 9:e113320. [PubMed: 25409328]
11. Bellani G, Laffey JG, Pham T, Fan E, Brochard L, Esteban A, et al. Epidemiology, Patterns of Care, and Mortality for Patients With Acute Respiratory Distress Syndrome in Intensive Care Units in 50 Countries. JAMA. 2016; 315:788–800. [PubMed: 26903337]
12. Matthay MA, Ware LB, Zimmerman GA. The acute respiratory distress syndrome. J Clin Invest. 2012; 122:2731–2740. [PubMed: 22850883]
13. Barth PJ, Höltermann W, Müller B. The spatial distribution of pulmonary lesions in severe ARDS. An autopsy study of 35 cases. Pathol Res Pract. 1998; 194:465–471. [PubMed: 9728363]
14. Pesenti A, Musch G, Lichtenstein D, Mojoli F, Amato MBP, Cinnella G, et al. Imaging in acute respiratory distress syndrome. Intensive Care Med. 2016; 42:686–698. [PubMed: 27033882]
15. Wigenstam E, Rocksén D, Ekstrand-Hammarström B, Bucht A. Treatment with dexamethasone or liposome-encapsuled vitamin E provides beneficial effects after chemical-induced lung injury. Inhal Toxicol. 2009; 21:958–964. [PubMed: 19572781]

16. Herber-Jonat S, Mittal R, Gsinn S, Bohnenkamp H, Guenzi E, Schulze A. Comparison of lung accumulation of cationic liposomes in normal rats and LPS-treated rats. Inflamm Res. 2011; 60:245–253. [PubMed: 20938712]
17. Hegeman MA, Cobelens PM, Kamps J, Hennus MP, Jansen NJG, Schultz MJ, et al. Liposome-encapsulated dexamethasone attenuates ventilator-induced lung inflammation. Br J Pharmacol. 2011; 163:1048–1058. [PubMed: 21391981]
18. Hood ED, Greineder CF, Dodia C, Han J, Mesaros C, Shuvaev VV, et al. Antioxidant protection by PECAM-targeted delivery of a novel NADPH-oxidase inhibitor to the endothelium in vitro and in vivo. J Control Release. 2012; 163:161–169. [PubMed: 22974832]
19. Lin X, Barravecchia M, Kothari P, Young JL, Dean DA. β1-Na(+),K(+)-ATPase gene therapy upregulates tight junctions to rescue lipopolysaccharide-induced acute lung injury. Gene Ther. 2016; 23:489–499. [PubMed: 26910760]
20. Brenner JS, Greineder C, Shuvaev V, Muzykantov V. Endothelial nanomedicine for the treatment of pulmonary disease. Expert Opin Drug Deliv. 2015; 12:239–261. [PubMed: 25394760]
21. Preissler G, Loehe F, Huff IV, Ebersberger U, Shuvaev VV, Bittmann I, et al. Targeted endothelial delivery of nanosized catalase immunoconjugates protects lung grafts donated after cardiac death. Transplantation. 2011; 92:380–387. [PubMed: 21778930]
22. Fu P, Birukova AA, Xing J, Sammani S, Murley JS, Garcia JGN, et al. Amifostine reduces lung vascular permeability via suppression of inflammatory signalling. Eur Respir J. 2009; 33:612–624. [PubMed: 19010997]
23. Ferrer MCC, Shuvaev VV, Zern BJ, Composto RJ, Muzykantov VR, Eckmann DM. Icam-1 targeted nanogels loaded with dexamethasone alleviate pulmonary inflammation. PLoS One. 2014; 9:e102329. [PubMed: 25019304]
24. Hellewell PG, Young SK, Henson PM, Worthen GS. Paradoxic effect of ibuprofen on neutrophil accumulation in pulmonary and cutaneous inflammation. Am J Respir Crit Care Med. 1995; 151:1218–1227. [PubMed: 7697256]
25. Hellewell PG, Henson PM, Downey GP, Worthen GS. Control of local blood flow in pulmonary inflammation: role for neutrophils, PAF, and thromboxane. J Appl Physiol. 1991; 70:1184–1193. [PubMed: 2032984]
26. Gattinoni L, Caironi P, Valenza F, Carlesso E. The role of CT-scan studies for the diagnosis and therapy of acute respiratory distress syndrome. Clin Chest Med. 2006; 27:559–570. abstract vii. [PubMed: 17085245]
27. Cutaia M, Rounds S. Hypoxic pulmonary vasoconstriction. Physiologic significance, mechanism, and clinical relevance. Chest. 1990; 97:706–718. [PubMed: 2407454]
28. Sylvester JT, Shimoda LA, Aaronson PI, Ward JPT. Hypoxic pulmonary vasoconstriction. Physiol Rev. 2012; 92:367–520. [PubMed: 22298659]
29. Hadad N, Tuval L, Elgazar-Carmom V, Levy R, Levy R. Endothelial ICAM-1 protein induction is regulated by cytosolic phospholipase A2α via both NF-κB and CREB transcription factors. J Immunol. 2011; 186:1816–1827. [PubMed: 21199900]
30. Ellinghaus P, Perzborn E, Hauenschild P, Gerdes C, Heitmeier S, Visser M, et al. Expression of proinflammatory genes in human endothelial cells: Comparison of rivaroxaban and dabigatran. Thromb Res. 2016; 142:44–51. [PubMed: 27131284]

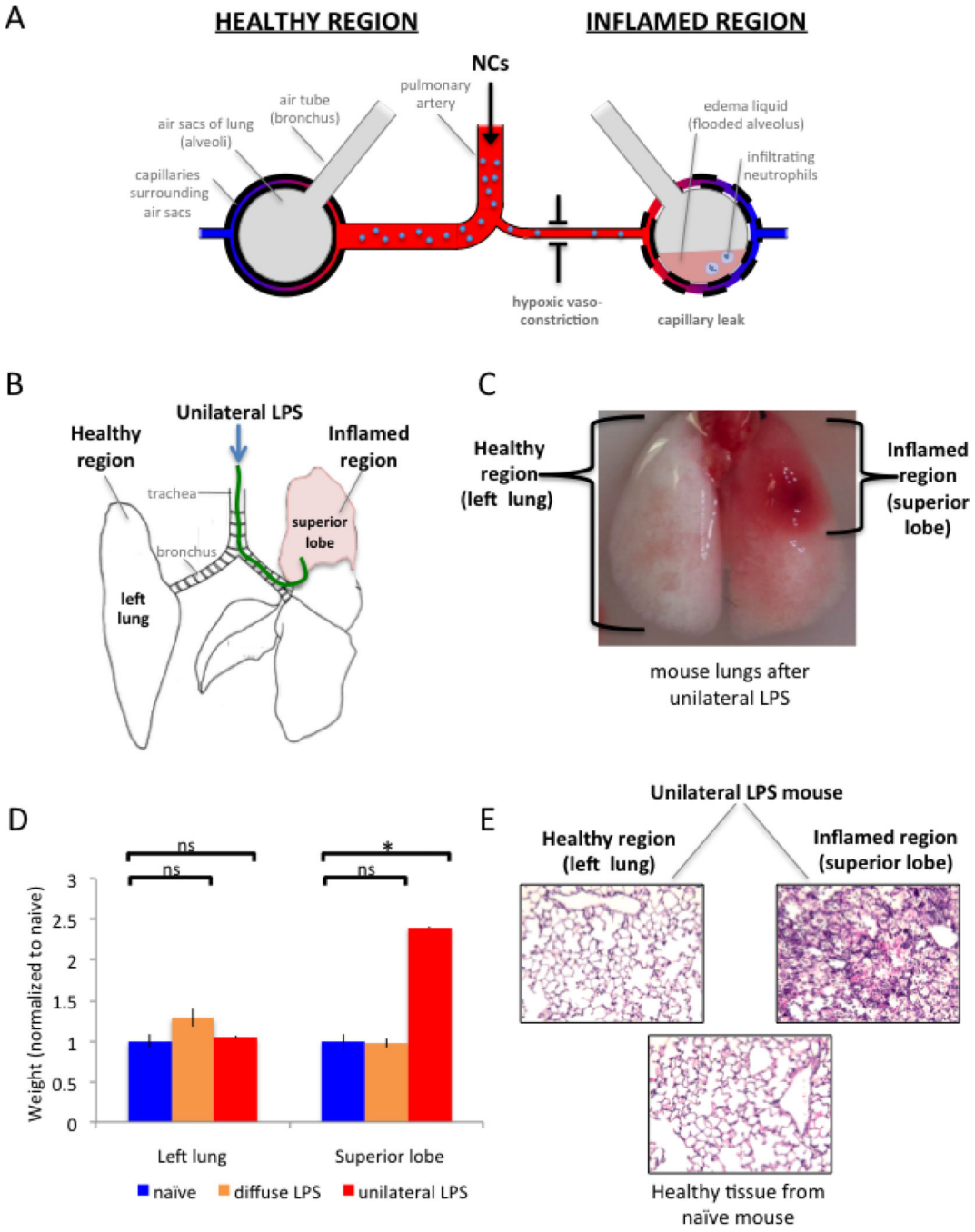

Figure 1. A new mouse model of ARDS for testing whether NCs preferentially distribute to inflamed or healthy lung regions

(A) Schematic of lungs in ARDS, with both healthy regions of lung tissue (*left side*) and inflamed regions (*right side*) in the same individual. IV-injected NCs reach the lung via the pulmonary artery (*center*), which has branches leading to each lung region. Lung regions are depicted as air sacs (*large grey circles*) surrounded by capillaries (*tubes with red-to-blue gradient*). The pathological region experiences hypoxic vasoconstriction (arteriolar narrowing), capillary leak (increased permeability of the capillaries), and filling of the air sacs with edema liquid (*pink*) and neutrophils. (B) Diagram of unilateral LPS instillation,

dorsal view. A custom 0.024” OD catheter (*green*) is threaded through the mouth and into the superior lobe, whereupon LPS is instilled. (C) Mouse lungs (dorsal view) that received unilateral LPS display a healthy region that is indistinguishable from naive (left lung; white), and a severely inflamed region (superior lobe; red). (D) To quantify the ARDS phenotype of edema liquid, we measured the weights of each lung region. Compared to naive (*blue bars*), the unilateral LPS model (*red bars*) displays no increased weight in the healthy region (left lung), but a 2.4-fold increase in weight of the inflamed region (superior lobe), due to edema liquid filling the air sacs of the inflamed region. The classical model of “diffuse LPS” (which is spatially homogeneous) (*orange bars*) displays no change in weight. (E) To observe the ARDS phenotype of neutrophilic infiltration, unilateral LPS mouse lungs were fixed and H&E-stained, which displays neutrophils as round purple cells. The healthy lung tissue (left lung) of these mice displays no neutrophilic infiltrate (*left panel*) when compared to a naive mouse (*bottom panel*), while the inflamed tissue (superior lobe) has every air sac filled with neutrophils (*right panel*). *, $p < 0.01$. ns, non-significant.

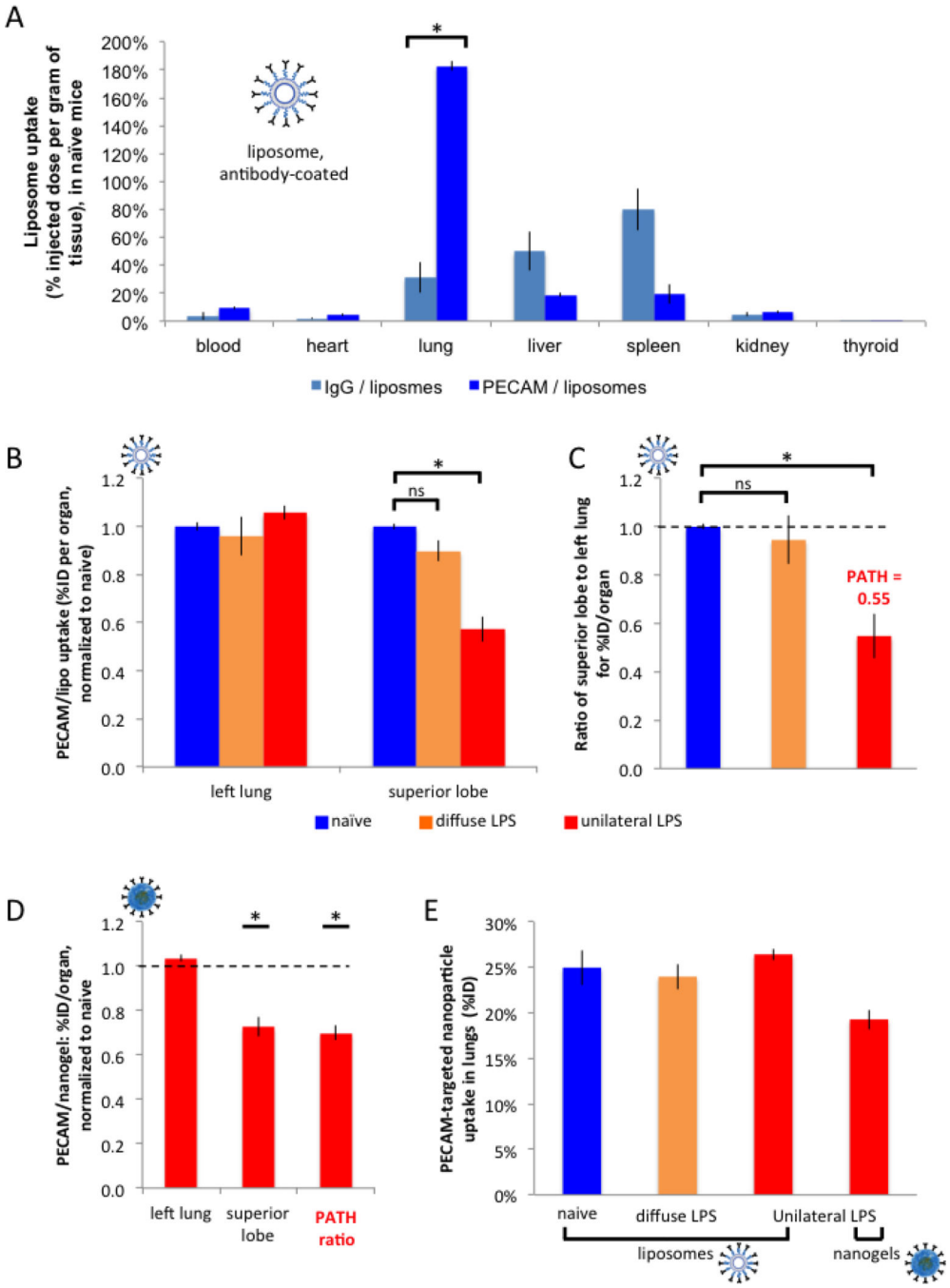

Figure 2. PECAM/NCs markedly concentrate in the lungs, but preferentially accumulate in healthy rather than inflamed lung tissue

(A) (A) Healthy (naïve) mice were IV-injected with liposomes (inset; labeled with I^{125}) conjugated to anti-PECAM antibodies or control antibodies, sacrificed 30 minutes later, and organ uptake was measured by gamma counter. Anti-PECAM liposomes display 5.9-fold higher lung concentratinos than control liposomes. (B) 24 hours after either unilateral LPS (*red bars*), diffuse LPS (*orange*), or sham (naive; *blue*), mice were IV-injected with anti-PECAM-liposomes, sacrificed 30 minutes later, and then lung lobes were measured as in *A*. For each mouse, we calculated the ratio of superior lobe to left lung for the percent injected

dose (%ID) per organ (“organ” here being a lung lobe), and normalized to naive. (C) For each mouse, we calculated the ratio of superior lobe to left lung for the %ID/organ values in *B*, normalized to the value for naïve mice. Note that this ratio for unilateral LPS mice (*third bar*) is defined as the PATH ratio *(Pathologically Altered To Healthy ratio)*, which is the %ID/organ of the pathological (inflamed) tissue divided by the %ID/organ of the healthy tissue, normalized to naive. A PATH ratio < 1 (here it is 0.55), indicates that a NC preferentially accumulates in healthy tissue, while a PATH ratio > 1 implies preferential accumulation in pathological (inflamed) tissue. (D) With the same protocol as in *B* and *C*, unilateral LPS mice were injected with an alternative nanocarrier, nanogels, also coated with anti-PECAM antibodies, producing a similar PATH ratio < 1. Only values with unilateral LPS are displayed (*red bars*). (F) Replotting *A-D* as %ID shows no differences in *whole-lung* uptake of PECAM/NCs, regardless of the presence of LPS instillation. *, $p < 0.05$. ns, non-significant.

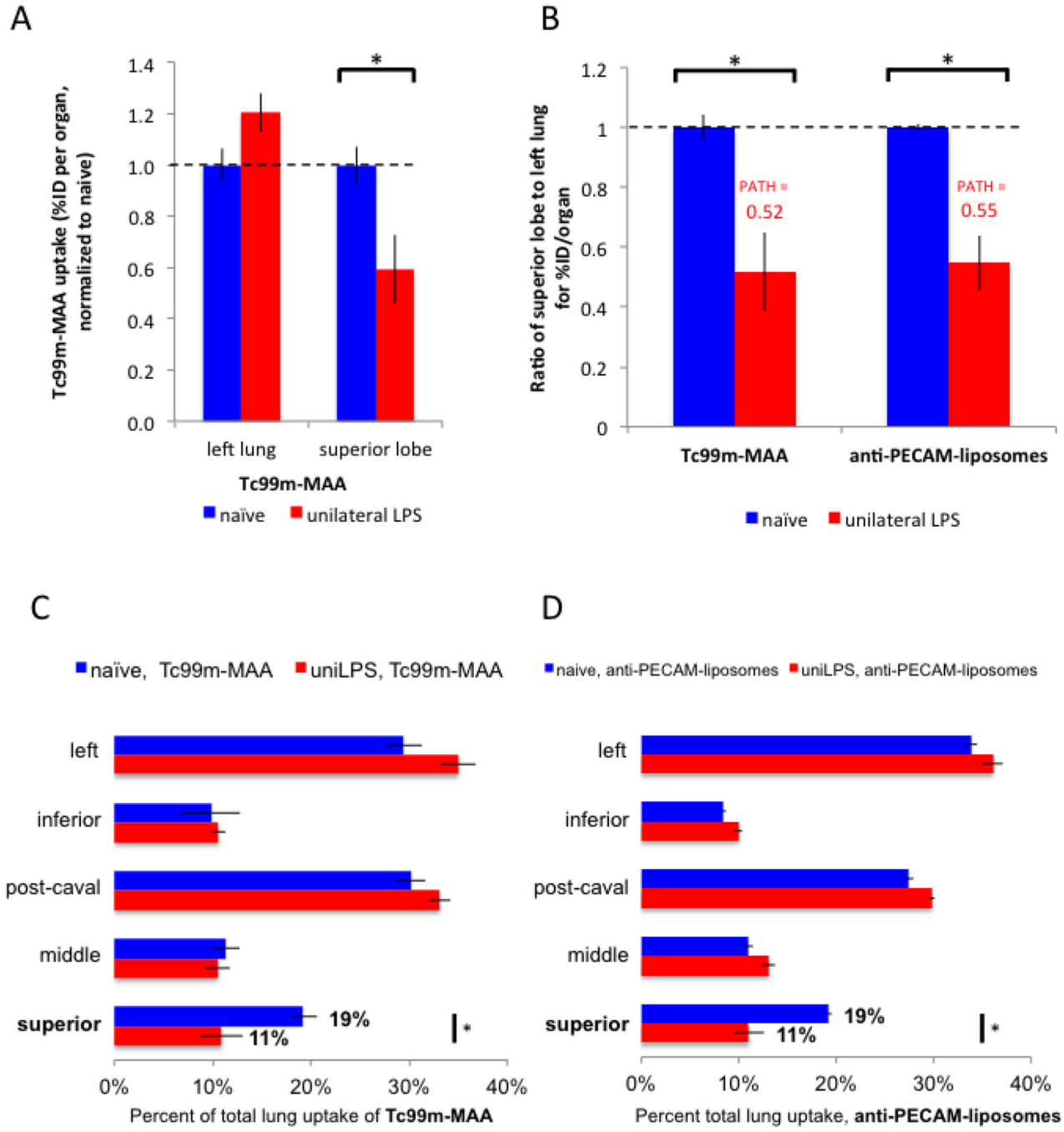

Figure 3. PECAM/NCs preferentially accumulate in the healthy lung regions because of hypoxic vasoconstriction in the inflamed regions

(A) Regional blood flow was measured by IV-injecting Tc^{99m}-MAA. The inflamed superior lobe of unilateral LPS mice displays reduced blood flow (lower Tc^{99m}-MAA / organ), likely to due hypoxic vasoconstriction. (B) Replotting the data of *A* as the ratio of superior lobe to left lung for %ID/organ (*first two bars*) and comparing this data to the same ratios obtained for PECAM/NCs (*third and fourth bars*). Note the two PATH ratios are nearly identical. (C and D) To display the correlation of blood flow and PECAM/NC distribution, all 5 lobes from the mice in *A* are displayed as % of total lung uptake. Mice injected with either Tc^{99m}-

MAA (C) or PECAM/NCs (D) display nearly identical patterns, particularly in the superior and left lobes. *, $p < 0.05$.

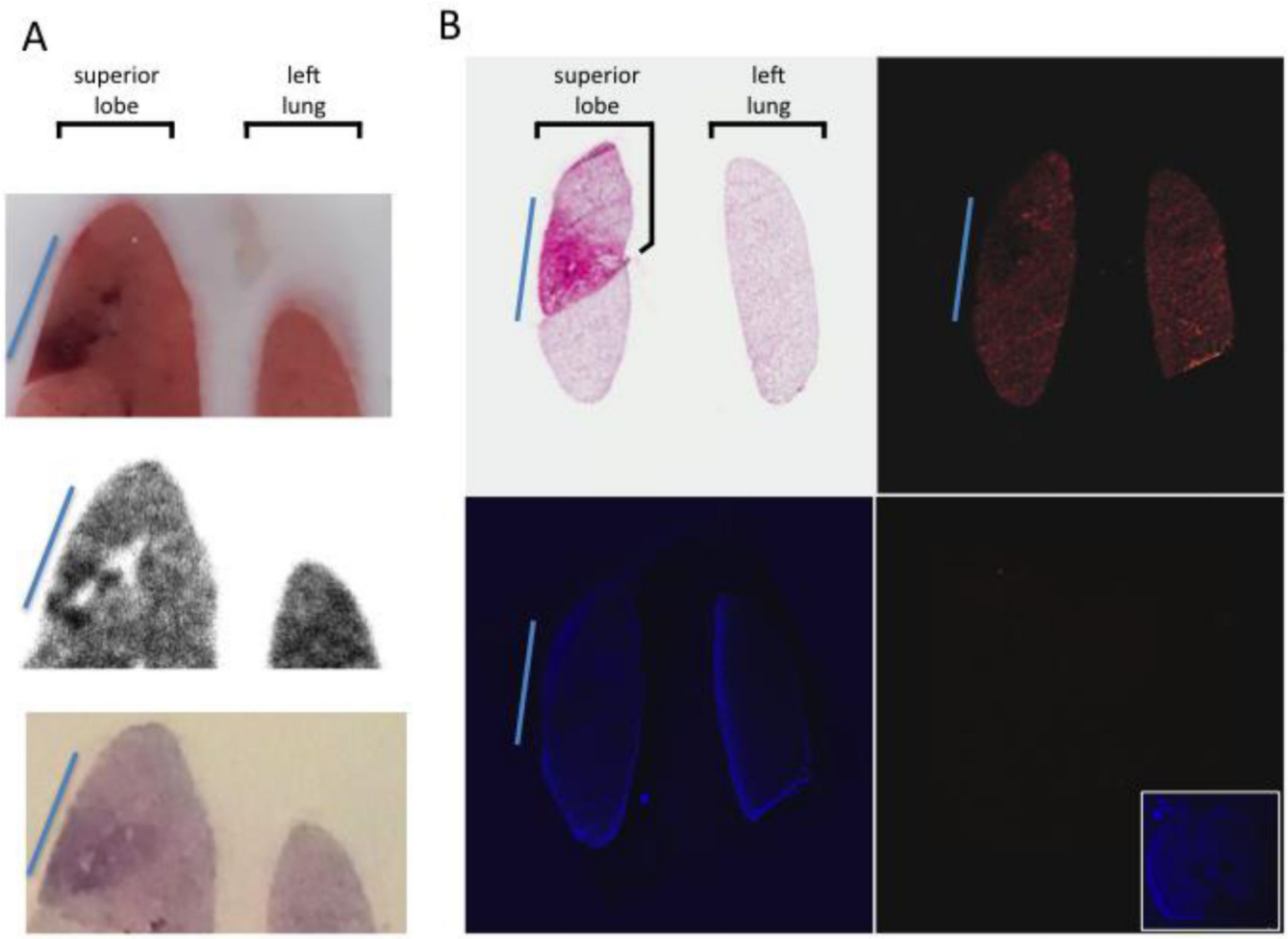

Figure 4. Within the inflamed lung lobe, sub-regions with the most severe inflammation receive the least PECAM/NCs

(A) At 24 hours after unilateral LPS instillation, mice were injected with In^{111}-labeled anti-PECAM-liposomes, and 30 minutes later lungs were removed and fresh-frozen. The *top panel* shows a slice of the tissue block, displaying a very clear sub-lobar inflammatory injury (*blue line*). DAR (*middle panel*) of the same slice shows the highly inflamed sub-region has portions with nearly no nanoparticle uptake (white holes) surrounded by other areas with very strong nanoparticle uptake (black). *Bottom panel*, H&E staining reveals intense neutrophilic infiltrates (dark purple) in this sub-region. (B) Similar protocol to *A*, but with rhodamine-labeled liposomes. *Top left*, H&E shows a sub-region of the superior lobe with severe inflammation (*blue line*). *Top right*, rhodamine signal the severely pathological sub-region (*blue line*) has less liposome uptake (less red signal) than the rest of the lobe. *Bottom left*, DAPI image. *Bottom right*, Image from an uninjected mouse displays nearly no signal with the same microscope settings as the top right panel, but normal DAPI signal (*inset*).

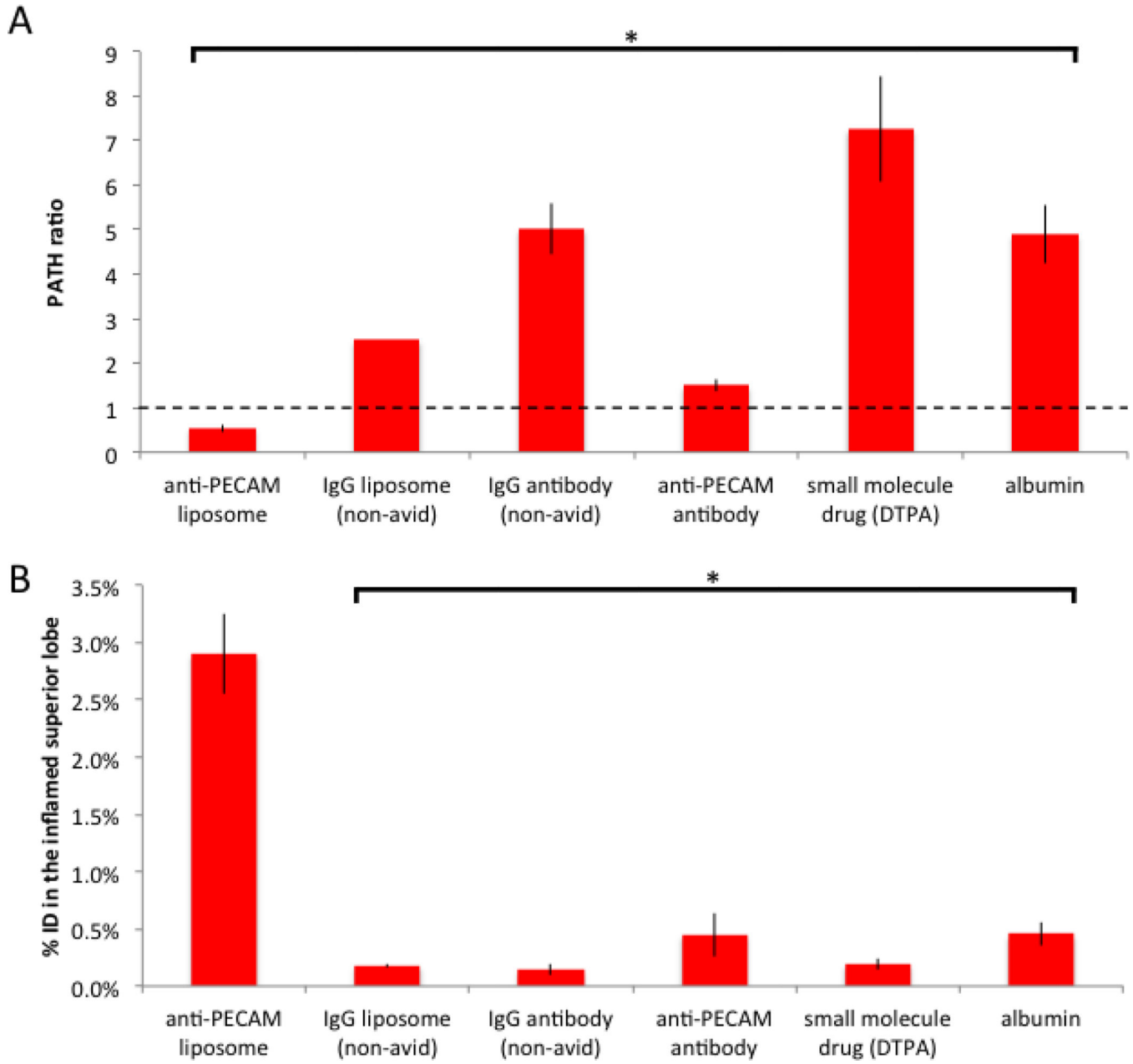

Figure 5. IgG/NCs, small molecule drugs, and proteins preferentially accumulate in the most inflamed tissue because of capillary leak

(A) The PATH ratio for unilateral LPS mice for a variety of pharmacological agents shows only PECAM/NCs have a PATH ratio < 1 (shunting away from the most inflamed lung tissue), while all others have PATH ratio values >1 (preferential accumulation in the most inflamed tissue). Note that radiolabeled albumin (*sixth bar in this plot*) is the gold-standard for measuring capillary leak, and its PATH ratio of 5 here fits with reported capillary leak metrics in severe ARDS. (B) Despite the high PATH ratios, these other agents have markedly lower *total mass* accumulating in the most inflamed region (superior lobe) than PECAM/NCs, due to the much higher total lung uptake of PECAM/NCs. *, $p < 0.01$. ns, non-significant. * indicates statistical comparison to naïve control.

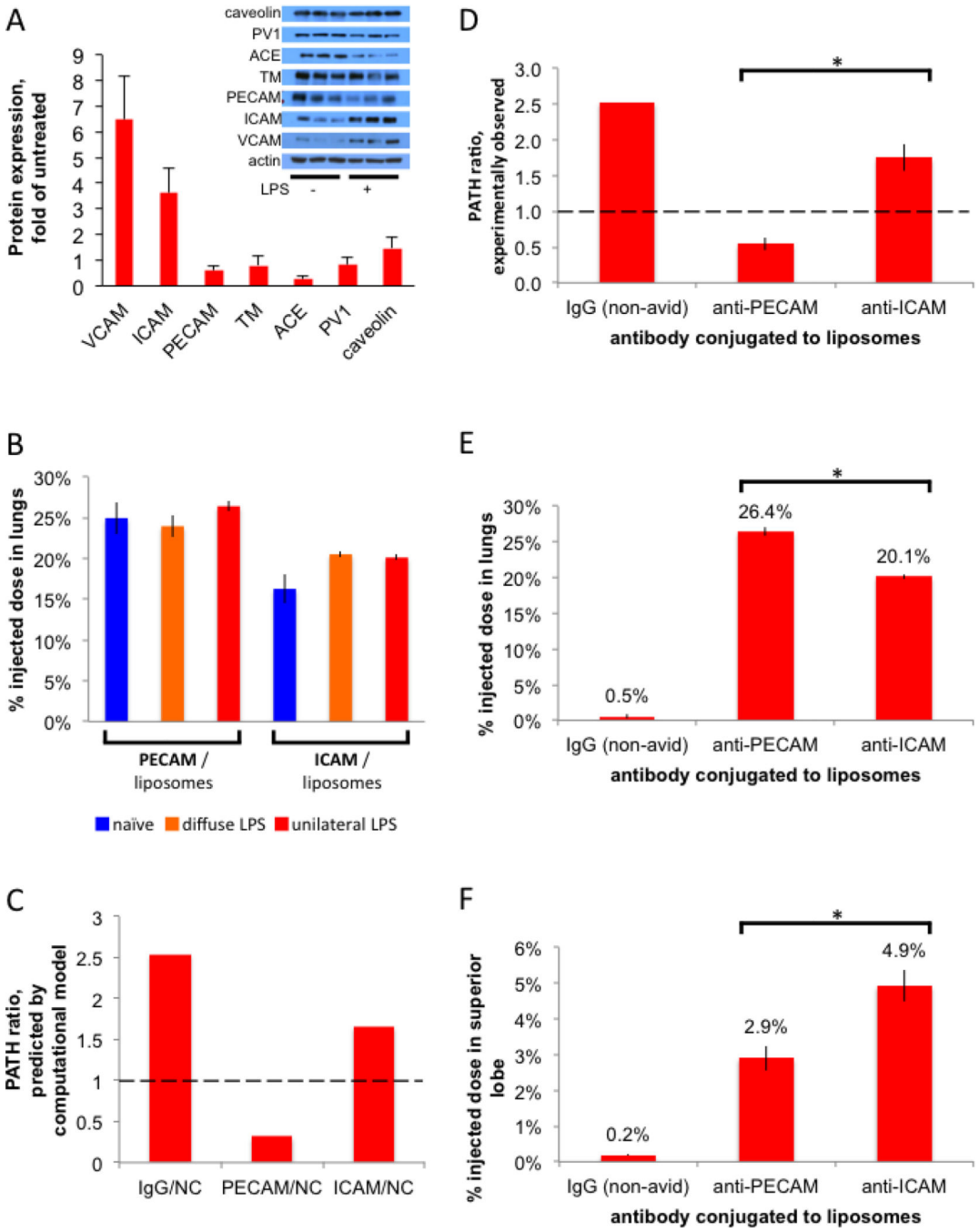

Figure 6. ICAM/NCs accumulate preferentially in inflamed lung regions because of increased epitope levels in that region

(A) A screen to identify targeting epitopes that are increased in the lungs of mice after LPS stimulation. *Inset*, Western blot of whole lung homogenates from either naive mice or mice given IV LPS 24 hours before sacrifice. Each lane represents an individual mouse, 3 mice per condition. The bar graph shows quantification of the *inset* Western, normalized to actin, and then mean of LPS mice was divided by the mean of naive mice. (B) ICAM/liposomes display increased (1.26x) whole-lung uptake in diffusely inflamed lungs, but still have lower (by 15%) whole-lung uptake than PECAM/liposomes. 24 hours after either unilateral LPS

(*red bars*), diffuse LPS (*orange*), or sham (naive; *blue*), mice were IV-injected with I^{125}-labeled liposomes and whole-lung uptake measured 30 minutes later. (C) A multi-compartment pharmacokinetic model (see Supplemental Materials), incorporating our measurements of hypoxic vasoconstriction, capillary leak, and epitope expression, predicts a PATH ratio < 1 for PECAM/NCs (*first red bar*) but a PATH ratio ~1 for ICAM/NCs. (D) Experimentally determined PATH ratios show that PECAM/NCs preferentially accumulate in healthy lung tissue (PATH ratio < 1), while ICAM/NCs are preferentially taken up into the inflamed superior lobe (PATH ratio > 1). (E) Whole-lung uptake, shows PECAM/NCs have the greatest total lung uptake. (F) Uptake in the just the intended target lobe, the severely inflamed superior lobe, with ICAM/NCs performing the best. *, $p < 0.05$.

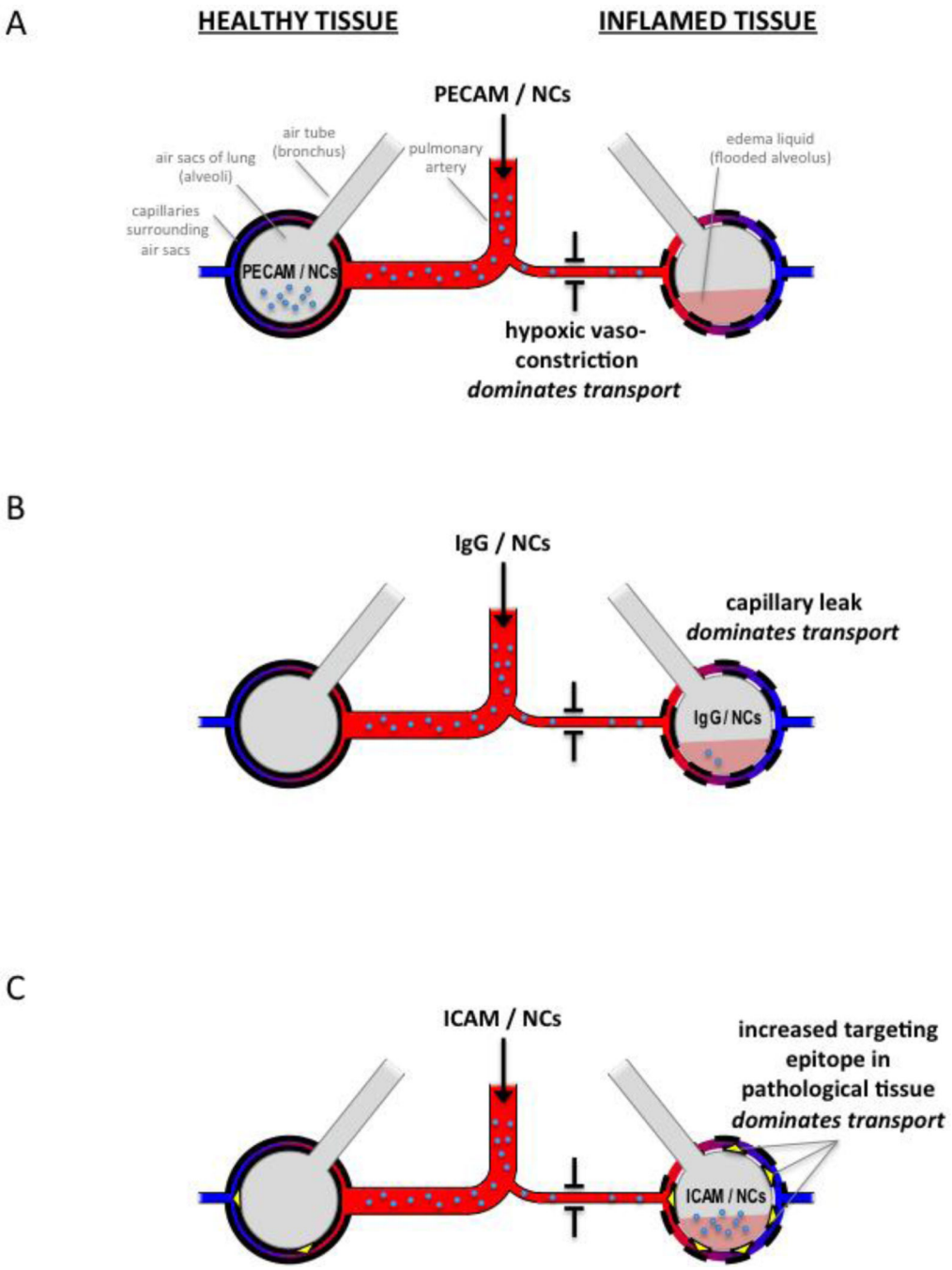

Figure 7. Three transport mechanisms determine relative distribution of NCs between healthy and inflamed lung regions

Inflamed tissue displays 3 changes that affect NC transport: hypoxic vasoconstriction (depicted as a narrow arteriole), capillary leak (depicted as dashed line of capillary walls), and increased ICAM epitope (yellow triangles in *C*). (A) PECAM/NCs (small blue circles) bind very rapidly to the capillary endothelium, and thus their distribution is determined by relative blood flow to each lung region. Therefore, PECAM/NC distribution is dominated by hypoxic vasoconstriction in inflamed lung tissue, resulting in preferential accumulation of PECAM/NCs in healthy tissue (depicted, for simplicity, as NCs in the air sac), which

implies a PATH ratio < 1. (B) IgG/NCs only accumulate in the lung where there is capillary leak, so capillary leak dominates distribution, resulting in IgG/NCs accumulating in the inflamed tissue (PATH ratio > 1). Compared to the avid lung binding of PECAM/NCs, the leak-induced lung accumulation of IgG/NCs is very low, depicted as relatively few NCs present in the lungs. (C) ICAM/NCs encounter more accessible ICAM epitopes in inflamed tissue, and this effect dominates over hypoxic vasoconstriction, resulting in preferential accumulation in the inflamed lung tissue (PATH ratio > 1). Additionally, ICAM/NCs benefit from avid lung binding, and thus have high levels of overall lung uptake (depicted as a large number of NCs in the lungs).